Photoionization mass spectrometry of ω-phenylalkylamines: Role of radical cation-π interaction

Davide Corinti, Daniele Catone, Stefano Turchini, Flaminia Rondino, Maria Elisa Crestoni, and Simonetta Fornarini

Citation: The Journal of Chemical Physics **148**, 164307 (2018); doi: 10.1063/1.5027786
View online: https://doi.org/10.1063/1.5027786
View Table of Contents: http://aip.scitation.org/toc/jcp/148/16
Published by the American Institute of Physics

Photoionization mass spectrometry of ω-phenylalkylamines: Role of radical cation-π interaction

Davide Corinti,[1] Daniele Catone,[2] Stefano Turchini,[2] Flaminia Rondino,[3] Maria Elisa Crestoni,[1] and Simonetta Fornarini[1,a)]

[1]*Dipartimento di Chimica e Tecnologie del Farmaco, Università di Roma "La Sapienza," P.le A. Moro 5, I-00185 Roma, Italy*

[2]*CNR-ISM, Area della Ricerca di Roma Tor Vergata, Via del Fosso del Cavaliere 100, Roma, Italy*

[3]*C. R. ENEA Frascati, FSN-TECFIS, Via E. Fermi 45, 00044 Frascati, Italy*

(Received 6 March 2018; accepted 9 April 2018; published online 26 April 2018)

Linear ω-phenylalkylamines of increasing alkyl chain length have been investigated employing synchrotron radiation in the photon energy range from 7 to 15 eV. These molecules have received considerable interest because they bear the skeleton of biologically relevant compounds including neurotransmitters and because of the possible interaction between the amino moiety and the phenyl ring. Recently, the contribution of this interaction has been assayed in both neutral and protonated species, pointing to a role of the polymethylene chain length. In this work, the ionization energy (IE) values of benzylamine (BA), 2-phenylethylamine (2-PEA), 3-phenylpropylamine (3-PPA), and 4-phenylbutylamine (4-PBA) were investigated in order to ascertain the impact of the different alkyl chain lengths and to verify an amino radical cation–π interaction. The IEs obtained experimentally, 8.54, 8.37, 8.29, and 8.31 eV for BA, 2-PEA, 3-PPA and 4-PBA, respectively, show a decreasing trend that is discussed employing calculations at the CBS-QB3 level. Moreover, the appearance energy values for major fragments produced by the photofragmentation process are reported. *Published by AIP Publishing.* https://doi.org/10.1063/1.5027786

I. INTRODUCTION

Phenylalkylamines (PAAs) bearing a phenyl and an amino group on the terminal carbon atoms of a linear (poly)methylene chain ($C_6H_5(CH_2)_nNH_2$, ω-phenylalkylamines) include parent molecules of important families of compounds such as the ethylamino neurotransmitters.[1] Depending on the number of methylene units (n), the end functional groups may be allowed to interact, taking advantage of the flexible character of the linker. The ensuing structural and dynamical properties represent simplified models of interactions occurring in more complex biomolecular systems. In particular, isolated molecular constituents in the gas phase lend themselves to reveal intrinsic factors that affect functionality in biological networks. In this view, several spectroscopic studies have addressed the conformational landscape of gaseous 2-phenylethylamine (2-PEA, $C_6H_5(CH_2)_2NH_2$), the simplest member of aromatic neurotransmitter molecules which include dopamine and amphetamine.[2] 2-Phenylethylamine (2-PEA) conformers present either an extended arrangement of the ethylamino ($H_2N(CH_2)_2$—) side chain with the NH_2 group pointing away (*anti*) from the phenyl group or a folded conformation where NH_2 is in a *gauche*-type relation relative to the phenyl ring. The ensuing structures are grouped in Fig. 1 including the relative zero point corrected electronic energies as reported at the MP2/6-311++G(d,p) level.[3] The two most stable gauche conformers G1 and G2 are stabilized by a NH···π interaction which is missing in G3 due to the orientation of the NH bonds away from the phenyl ring. Conformers G1 and G2 have been detected and their shape determined by microwave spectroscopy.[4]

The rotational spectra of both G1/G2 and A1/A2 have been recorded using molecular beam Fourier transform microwave spectroscopy, while G3 is not sampled in the supersonic expansion, likely due to selective collisional relaxation of this species to G1.[3] Previous studies on the conformation and electronic spectroscopy of 2-PEA and more recent work using *ab initio* calculations, fluorescence spectroscopy, and mass spectrometry are consistent with these results.[5–9] Also ionization loss Raman spectra combined with quantum chemical calculations have confirmed the presence of four conformers.[10,11]

When the basic amino group of 2-PEA is protonated, the interaction between the so-formed alkylammonium ion and the phenyl ring becomes a significant contribution to the relative stability of the possible conformational structures. The folded conformer allowing the $NH^+\cdots\pi$ interaction is found to be ca. 20 kJ mol^{-1} lower in energy relative to the extended anti-conformation, according to *ab initio* calculations at the ωB97X-D/6-311++G(d,p) level.[12] The theoretical results are consistent with a thorough assay of protonated 2-PEA ions as isolated gaseous species, based on IR multiple photon dissociation (IRMPD) spectroscopy. In particular, a distinct vibrational signature at 3143 cm^{-1} is reported to characterize the stretching mode of the NH bond involved in the π interaction, significantly red-shifted with respect to the "free"

a)Author to whom correspondence should be addressed: simonetta.fornarini@uniroma1.it

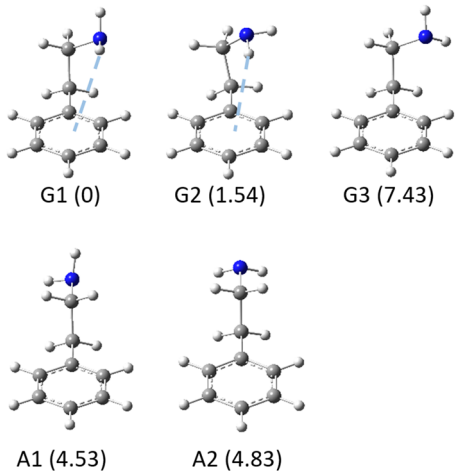

FIG. 1. Gauche (G1-G3) and anti-(A1, A2) conformers of 2-phenylethylamine (2-PEA).[3] Relative energies (in kJ mol^{-1}) are calculated at the MP2/6-311++G(d,p) level and include zero point correction.[3]

NH stretching modes at 3307 and 3351 cm^{-1}.[12] Infrared photon dissociation (IRPD) spectroscopy and rare gas tagging of cold ions have also been exploited to reveal geometric and vibrational properties of protonated 2-PEA and related neurotransmitters.[1,13,14] The amino acid phenylalanine is a molecule closely related to 2-PEA, bearing an additional carboxylic group (—CO_2H) on the amino-substituted carbon. Not surprisingly, protonated phenylalanine shows clear evidence of cation-π interactions between the protonated amino group and the aromatic ring as shown by the vibrational signatures of the naked species.[15–17]

Whereas cation-π interactions are widely documented non-covalent forces, the open shell version, namely, radical cation-π ($RC^{+\bullet}$-π) interactions, has received much less consideration.[18–20] Energetic and geometric characteristics of $RC^{+\bullet}$-π interactions have been described using computational tools. The $RC^{+\bullet}$-π interaction has resulted to be energetically more favorable than the cation-π interaction and the spin density found to reside basically on the aromatic ring. The interaction energy of the $NH_3{}^{+\bullet}$-benzene complex is calculated at 85 kJ mol^{-1}, corresponding to a structure where the N atom is centered above the aromatic ring and the three hydrogen atoms point away from the ring. In this geometry, a significant extent of electron transfer has taken place as shown by molecular orbital and spin density analyses.[18]

In this contribution, photoionization mass spectrometry in the vacuum ultraviolet (VUV) region is performed on ω-phenylalkylamines, $C_6H_5(CH_2)_nNH_2$ with n varying from one to four (Scheme 1). The interest placed in this family of molecules resides in their differing flexibility and in the potential approach of the phenyl and amino group which may be expected to affect their properties. Previous studies combining an experimental and theoretical survey of appearance energies (AEs) have provided valuable information on specific effects due to varying structures.[21] A similar approach, based on a VUV synchrotron beamline, is pursued in the present contribution.

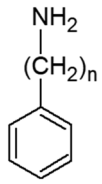

n	Species
1	benzylamine
2	2-phenylethylamine
3	3-phenylpropylamine
4	4-phenylbutylamine

SCHEME 1. Schematic representation of the sampled ω-phenylalkylamines.

II. METHODS

A. VUV photodissociation experiments

Benzylamine (BA), 2-phenylethylamine (2-PEA), 3-phenylpropylamine (3-PPA), and 4-phenylbutylamine (4-PBA), collectively shown in Scheme 1, are commercial products. The pure substances are liquid at room temperature and were purified by repeated evaporation/condensation cycles. They were placed in a test tube connected to the gas line of the vacuum chamber and admitted in the chamber in vapor phase through a needle. The experiments were performed at the "Circular Polarization" (CiPo) beamline 4.2 at the Elettra synchrotron facility (Trieste, Italy).[22] The energy of the synchrotron radiation was selected by an aluminium normal incidence monochromator (NIM) that covers the photon energy range 5–17 eV with a resolving power of about 1000. The setup of the chamber consists of five electrostatic lenses that focus and accelerate the ions from the region of interaction to the quadrupole mass spectrometer (10-4000 u, Extrel 150-QC 0.88 MHz), mounted perpendicular to the photon beam and to the effusive gas beam. A detailed overview of the instrumental apparatus is reported in previous studies.[21,23]

Photoionization efficiency curves (PECs) for the selected ions were obtained from 7 to 15 eV of photon energy scanned in steps of 20 meV with an acquisition time of about 1 to 5 s/point, depending on the intensity of the assayed ion. Photon fluency was measured during each run employing a photodiode in order to normalize the PECs. To inspect the region up to 11.7 eV, a lithium fluoride filter was used, thus removing the second-order contribution of NIM. Above this threshold, the influence of second-order radiation was evaluated through the analysis of the argon atom photoionization efficiency curve. The ionization energy (IE) of argon, 15.76 eV, is in fact above the inspected VUV region. Therefore any Ar^+ ions may only be generated by the second-order radiation of the first-order photons in the 11.7–15.6 eV range, which allows to correlate the intensity of the Ar^+ signal with the incursion of second-order photons. Subsequently, these data have been used to correct the PEC of the fragment ions in order to obtain their appearance energy (AE) values. In addition, mass spectra of the selected species were recorded at 15 eV of photon energy.

B. Computational methods

The set of neutral ω-phenylalkylamine conformers presented in Secs. III B and III C was chosen following a computational procedure which involves progressive steps of optimization and subsequent selection of the lowest lying conformers, while increasing the accuracy of the computational method. A preliminary exploration of the ω-phenylalkylamine conformer population was performed using the conformer distribution tool as implemented in the Spartan'16 suite,

employing molecular mechanics as the computational method.[25]

With regard to 2-PEA, we also relied for the selection of the guess geometries on the work by Alonso *et al.* in which the authors analyze the 2-PEA conformers by theoretical calculations and microwave spectroscopy.[3] Subsequently, the selected geometries were optimized at the B3LYP/6-31+G* level of theory using Gaussian09 Rev. D01.[26] Vibrational modes were computed at the same level of theory to confirm the stationary states found as local minima. The lowest lying conformers of neutral ω-phenylalkylamines together with structures at higher energy, but representative of peculiar structural motifs, were treated with the CBS-QB3 composite method.[27] It includes a preliminary optimization at the B3LYP/6-311G(2d,d,p) level followed by a series of single point calculations involving post-Hartree-Fock methods. Furthermore, the neutral geometries were used as starting point to obtain the corresponding radical cations of BA, 2-PEA, 3-PPA, and 4-PBA. The restricted open-shell version of CBS-QB3 (ROCBS-QB3) was used for the radical cations in order to avoid the influence of spin contamination.[28] Finally to obtain the vertical IEs of the neutral conformers previously sampled, the ROCBS-QB3 method was employed without geometry optimization of the neutral geometries, imposing positive charge and doublet electronic state. From now on, for the sake of simplicity, we will uniformly use the denomination CBS-QB3 for both the restricted and restricted open versions of the method.

III. RESULTS AND DISCUSSION

A. VUV photodissociation of ω-phenylalkylamines

The selected ω-phenylalkylamines were ionized by VUV radiation with an energy ranging from 7 to 15 eV, leading to the respective radical cations and fragment ions. Figure 2 shows the PEC for the ionization of 2-PEA (2-PEA$^{+\bullet}$), as a function of the photon energy, together with zoomed data in a semilogarithmic scale reported in the inset.

The IE value is obtained from the intersection point of the linear fitting of the PEC in the threshold region with the background signal, as reported in previous papers.[22,29] A conservative estimate of ±0.05 eV error range is associated with the experimental determinations, mainly reflecting the bandwidth of the monochromator and the uncertainty of the ionization threshold as determined from the PEC. Thus, the IE of 2-PEA is obtained as 8.37 ± 0.05 eV. The same procedure was employed to evaluate the IEs of the other ω-phenylalkylamines, yielding values of 8.54 ± 0.05 eV, 8.29 ± 0.05 eV, and 8.31 ± 0.05 eV for BA, 3-PPA, and 4-PBA, respectively. The corresponding PECs are reported in Fig. S1 of the supplementary material. The consistency of the employed procedure is validated by the good agreement of the IE of BA obtained in this work with the value of 8.58 eV obtained by Xie *et al.*[29] using similar experimental conditions.

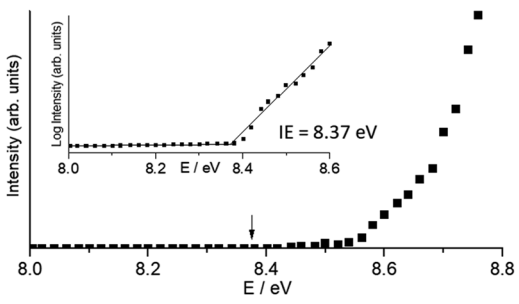

FIG. 2. PEC of 2-PEA$^{+\bullet}$ at *m/z* 121. The inset reports an expansion of the threshold region in a semi-logarithmic scale. The IE value is determined by the intersection between the lines fitting the background and the rising ion signal in the threshold region. The measured IE value is indicated by an arrow.

Increasing the photon energy above the IE, the formation of the radical cation is accompanied by extensive fragmentation. Figure 3 shows the mass spectra of BA, 2-PEA, 3-PPA, and 4-PBA acquired at 15 eV, and Fig. S2 of the supplementary material displays the PECs of the most abundant fragments. A more detailed discussion of the observed fragmentation paths is reported in the following paragraphs.

1. Benzylamine

In panel (a) of Fig. 3, the mass spectrum of BA acquired at 15 eV of photon energy is reported. The most abundant fragment is the ion at *m/z* 106, formed by loss of a hydrogen atom from the molecular radical cation. Other important fragmentation products are the ions at *m/z* 91, *m/z* 79, *m/z* 78, and *m/z* 30. The signal at *m/z* 17 corresponds to the radical cation of ammonia that is present as a contaminant in the sample, as confirmed comparing the AE of the ion with the IE of ammonia reported in the literature (10.07 ± 0.01 eV).[30] The fragmentation pattern of BA was previously described by Wittig *et al.* using a variety of ionization/activation techniques, including electron ionization (EI), IR multiple photon absorption, and UV multiphoton absorption.[31] Intriguingly, significant alterations in the fragmentation pattern of the ions generated by the three different techniques are reported. These dissimilarities are suggested to arise from the different kinetics of the

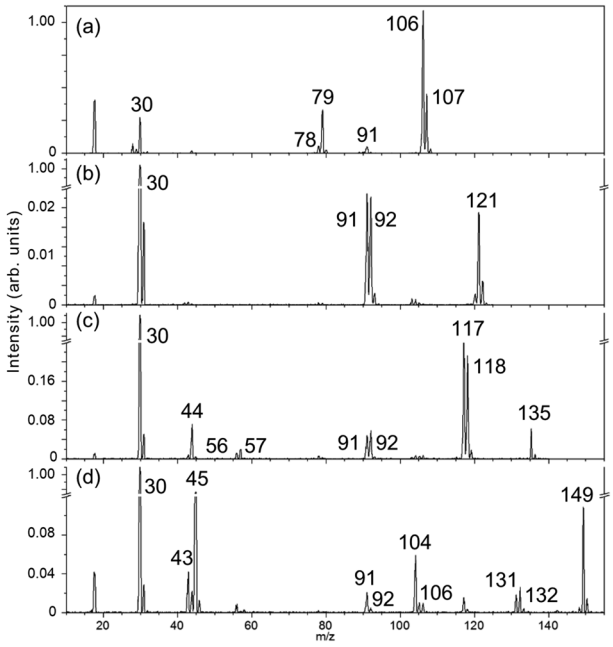

FIG. 3. Mass spectra of (a) BA (molecular ion at *m/z* 107), (b) 2-PEA (*m/z* 121), (c) 3-PPA (*m/z* 135), and (d) 4-PBA (*m/z* 149) acquired at 15 eV photon energy. The break in the y-axis is meant to emphasize the less intense signals.

three heating processes. A major difference lies in the absence of the fragment at *m/z* 30 in the mass spectrum obtained by IR multiple photon absorption, which is instead present in the EI spectrum at 23 and 50 eV. The observation of a significant abundance of the fragment at *m/z* 30 in the mass spectrum reported in Fig. 3(a) suggests that the photo-absorption process in the present experimental setup is comparable with EI, as far as the pattern of fragment ions is concerned. This behavior has been explained by the different activation regime. IRMPD, a "slow" activation process, leads selectively to the lowest energy fragmentation products. By contrast, UV multiphoton absorption drives higher energy paths such as hydrogen atom loss, whose occurrence precludes the formation of the m/z 30 ion. The AEs of the assayed fragments together with the formal attribution and the corresponding neutral loss are reported in Table I. The AE of the *m/z* 106 fragment observed at 9.05 ± 0.05 eV is in fair agreement with the value of 9.14 eV reported in the literature.[29]

TABLE I. Appearance energies of BA, 2-PEA, 3-PPA, and 4-PBA product ions. Ion and neutral formulas are reported.

Benzylamine (*m/z* 107)			
m/z	AE (eV)[a]	Neutral loss	Product ion composition
106	9.05	H	C_7H_8N
91	11.28	NH_2	C_7H_7
79	11.66	CH_2N	C_6H_7
78	10.58	CH_3N	C_6H_6
30	10.22	C_6H_5	CH_4N
2-phenylethylamine (*m/z* 121)			
m/z	AE (eV)[a]	Neutral loss	Product ion composition
92	9.58	CH_3N	C_7H_8
91	11.77	CH_4N	C_7H_7
30	8.63	C_7H_7	CH_4N
3-phenylpropylamine (*m/z* 135)			
m/z	AE (eV)[a]	Neutral loss	Product ion composition
118	8.63	NH_3	C_9H_{10}
117	10.62	NH_4	C_9H_9
92	10.59	C_2H_5N	C_7H_8
91	11.78	C_2H_6N	C_7H_7
57	9.34	C_6H_6	C_3H_7N
56	11.17	C_6H_7	C_3H_6N
44	8.85	C_7H_7	C_2H_6N
30	8.91	C_8H_9	CH_4N
4-phenylbutylamine (*m/z* 149)			
m/z	AE (eV)[a]	Neutral loss	Product ion composition
132	8.64	NH_3	$C_{10}H_{12}$
131	10.73	NH_4	$C_{10}H_{11}$
106	8.67	C_2H_5N	C_8H_{10}
104	9.11	C_2H_7N	C_8H_8
92	10.75	C_3H_7N	C_7H_8
91	10.92	C_3H_8N	C_7H_7
45	8.83	C_8H_8	C_2H_7N
43	9.38	C_8H_{10}	C_2H_5N
30	9.00	C_9H_{11}	CH_4N

[a]An error range of ±0.05 eV is associated with the experimental AEs.

2. 2-phenylethylamine

The mass spectrum of 2-PEA, reported in Fig. 3(b), shows relatively few fragments and is dominated by the ion at *m/z* 30 that has by far the highest intensity. The AE of the ion at *m/z* 30 (8.63 eV ± 0.05 eV), formally $CH_2{=}NH_2^+$, is also remarkable, being the lowest among all the fragments and just 0.26 eV higher than the IE of 2-PEA. The other two signals at *m/z* 92 ($C_7H_8^{+\bullet}$) and *m/z* 91 ($C_7H_7^+$) present AEs at 9.58 ± 0.05 eV and 11.77 ± 0.05 eV, respectively. The fragment at *m/z* 91 is likely to arise from hydrogen atom loss from the ion at *m/z* 92 rather than ensue by a direct C—C bond cleavage. In fact, in the latter case, the formation of the $CH_2NH_2^+$ cation is expected to be highly favored, on considering that the relative IEs of the $C_6H_5CH_2^{\cdot}$ and $NH_2CH_2^{\cdot}$ radicals are 7.24 eV and 6.29 eV, respectively.[32,33]

3. 3-phenyl-propylamine

The mass spectrum of 3-PPA reported in Fig. 3(c) presents a rich fragmentation pattern when compared to the mass spectra of the lighter ω-phenylalkylamines, although sharing some features in common. In particular, the presence of the most abundant fragment at *m/z* 30 has to be highlighted. Also fragment ions at *m/z* 91 and 92 are observed. Compared to the AE of $CH_2NH_2^+$ from 2-PEA, 3-PPA presents a higher AE for the same ion, namely, at 8.91 ± 0.05 eV, as reported in Table I. The fragment ions at *m/z* 92 and 91 present AEs of 10.59 ± 0.05 eV and 11.78 ± 0.05 eV, respectively. Once again, the lower AE of the *m/z* 92 ion with respect to the one at *m/z* 91 is confirmed, which may be compatible with a consecutive dissociation linking the two species. As a novel feature, it is now observed a fragment ion arising from the loss of ammonia at *m/z* 118, characterized by an AE value of 8.63 ± 0.05 eV. This dissociation channel is followed by the loss of a hydrogen atom generating the fragment at *m/z* 117 with an AE of 10.52 ± 0.05 eV. There are also lighter fragmentation products, in particular, the ions at *m/z* 44, 56, and 57 presenting an AE of 8.85 ± 0.05 eV, 11.17 ± 0.05 eV, and 9.34 ± 0.05 eV, respectively. These species arise from C—C bond cleavages occurring at different sections in the alkyl chain with the charge retained by the amino containing moiety ($C_2H_6N^+$, $C_3H_6N^+$, and $C_3H_7N^{+\bullet}$, respectively).

4. 4-phenyl-butylamine

The dissociation pattern of 4-PBA at 15 eV presents similarities with 3-PPA as reported in Fig. 3(d) and Table I. The predominance of the fragment at *m/z* 30 is confirmed. The reported AE of 9.00 eV for the ion at *m/z* 30 suggests a fragmentation process of similar energy requirements as the one occurring from the 3-PPA radical cation. In fact, the excess energy required to form $CH_2NH_2^+$ from the molecular ion of 3-PPA and 4-PBA is almost the same, being 0.62 eV and 0.69 eV (namely, the difference between IE and AE values reported in Table I), respectively. The fragmentation products related to $C_7H_8^{+\bullet}$ (*m/z* 92) and $C_7H_7^+$ (*m/z* 91) are also present and are characterized by AEs of 10.75 ± 0.05 eV and 10.92 ± 0.05 eV, respectively.

As discussed in the previous paragraph, it is interesting to note that the loss of ammonia is the dissociation channel presenting the lowest AE, i.e., 8.66 ± 0.05 eV. It generates the

fragment at *m/z* 132 and, as observed in the 3-PPA sample, the ion at *m/z* 132 loses a hydrogen atom yielding an ion at *m/z* 131 with an AE of 10.73 ± 0.05 eV. The mass spectrum of 4-PBA also includes fragment ions at *m/z* 45, 43, 106, and 104. Among these ones, the ion at *m/z* 45, formally $C_2H_7N^{+\bullet}$, is the second most intense signal of the spectrum and presents an AE of 8.83 ± 0.05 eV. A subsequent loss of H_2 could be related to the signal at *m/z* 43 in agreement with the slightly higher AE of this ion (9.38 ± 0.05 eV). The same process seems to govern the behavior of the ion at *m/z* 106, formally $C_8H_{10}{}^{+\bullet}$, presenting an AE of 8.66 ± 0.05 eV. In fact, the related species at *m/z* 104 is consistent with H_2 loss from $C_8H_{10}{}^{+\bullet}$, linked to the higher AE of 9.11 ± 0.05 eV. This interpretation is supported by comparing the difference between the AEs of the ions at *m/z* 45 and *m/z* 106 and the ones of the dehydrogenated species at *m/z* 43 and *m/z* 104, which are 0.55 eV and 0.45 eV, respectively.

B. Theoretical investigation of neutral and cationic species

The observed IEs show a decreasing trend ranging from 8.54 ± 0.05 eV for BA to 8.29 ± 0.05 eV for 3-PPA. This last value is just about equal to the IE of 4-PBA at 8.31 ± 0.05 eV, while the IE of 2-PEA is placed in between at 8.37 ± 0.05 eV. The reported differences are not negligible considering the similar structure of the ω-phenylalkylamines examined. Therefore, theoretical calculations were performed at the CBS-QB3 level to aid in the interpretation of the experimental data. The sampled ω-phenylalkylamines may present several rotational conformers that can be gathered in two main groups. As already described in the Introduction with regard to 2-PEA,[3] the conformation of the alkyl chain allows us to discriminate between two families. In fact, the dihedral angle linking the amino nitrogen, the two methylene carbon atoms, and the ipso carbon of the phenyl group permits to distinguish between a *gauche*-conformation, allowing NH_2 to lean toward the aromatic ring, and an *anti*-conformation, where the amino group is far from the phenyl group.[3] The same argument can be applied to 3-PPA and 4-PBA. In these cases, the longer alkyl chain does not allow selecting a single dihedral angle distinguishing two families, but one may still compare either elongated or compact conformers, where the amino-phenyl proximity is verified only in the latter ones. In the cited work,[3] the four experimentally observed conformers of 2-PEA lie within an energy range of 4.9 kJ mol^{-1} and the most stable species is the *gauche* one with the amino hydrogen directed toward the phenyl group (namely, G1 in Fig. 1), as also confirmed by the presently adopted computational method. Calculations run on the other neutral species (BA, 3-PPA, and 4-PBA) confirm that the conformational changes have a relatively small impact on the relative energies, leading to an utmost span of 5.2 kJ mol^{-1}. Optimized geometries of representative conformers for the sampled ω-phenylalkylamines are displayed in Fig. 4. Geometries depicting the same compound are grouped together and ordered according to their increasing zero point energy (ZPE) corrected electronic energy. Thus, for example, G1 and A1 conformers of 2-PEA (Fig. 1)[3] are named here **PEA1** and **PEA2**, respectively. Concerning 3-PPA and 4-PBA, it is interesting to note that the lowest lying conformers do not present the amino group oriented toward the ring. Apparently,

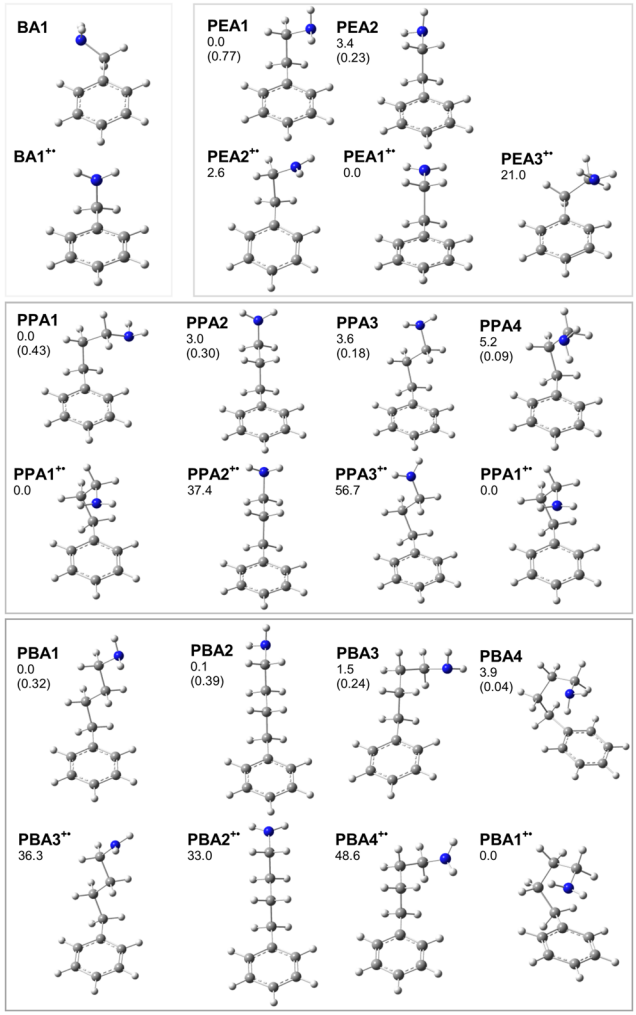

FIG. 4. Geometries of the representative species calculated at the CBS-QB3 level of theory. Relative ZPE corrected electronic energies for neutral and cationic species are reported in kJ mol^{-1} and are referred to the most stable conformer within each set. Progressive numbering within each set goes in parallel with increasing energy. In parentheses are reported the Boltzmann population fractions of the neutral species, calculated from relative free energies at 298 K, expected for thermal equilibration of the conformers at the temperature of the experiment.

the small energetic profit gained from the amino hydrogen-π interaction is not enough to outweigh the destabilization due to the associated unfavourable arrangement (tending to eclipsed configurations) of the methylene units. Thermodynamic data for the whole set of optimized structures shown in Fig. 4 are summarized in Table II.

A set of representative structures for the radical cations of the selected PPAs is reported in Fig. 4. In order to directly relate each neutral conformer with the radical cation presumably formed in the photoionization transition, ionized species are optimized from the starting neutral geometry once an electron has been removed and the so-obtained structures are presented one below the other, so maintaining their linked origin. The progressive numbering of radical cation structures once again reflects an increasing energy ordering. The conformers of PAA radical cations displayed in Fig. 4 comprise geometries presenting either an elongated or a compact structure. Here, the energy spread is distinctly wider within each conformational landscape. In fact, there are large differences in energy between

TABLE II. Thermodynamic data calculated at the CBS-QB3 level for neutral and ionized PAA conformers.

	EE[a]	EE_{rel}[b]	H_{rel} (298 K)[b]	G_{rel} (298 K)[b]
BA1	−326.278 871	0.0	0.0	0.0
BA1$^+$	−325.966 463	819.6	820.2	818.1
PEA1	−365.514 541	0.0	0.0	0.0
PEA2	−365.513 231	3.4	3.7	3.1
PEA1$^{+\bullet}$	−365.206 997	807.5	808.5	805.6
PEA2$^{+\bullet}$	−365.206 005	810.1	811.2	808.2
PEA3$^{+\bullet}$	−365.198 984	828.5	828.3	828.8
PPA1	−404.739 967	0.0	0.0	0.0
PPA2	−404.738 827	3.0	3.6	1.1
PPA3	−404.738 602	3.6	3.9	2.6
PPA4	−404.737 994	5.2	5.4	4.6
PPA1$^{+\bullet}$	−404.446 121	771.5	771.2	772.6
PPA2$^{+\bullet}$	−404.431 858	808.9	810.5	805.9
PPA3$^{+\bullet}$	−404.424 505	828.2	829.9	824.6
PBA1	−443.964 955	0.0	0.0	0.0
PBA2	−443.964 921	0.1	0.5	−0.6
PBA3	−443.964 384	1.5	1.4	0.9
PBA4	−443.963 452	3.9	3.4	6.5
PBA1$^{+\bullet}$	−443.666 573	783.4	782.3	788.0
PBA2$^{+\bullet}$	−443.653 994	816.4	817.9	814.1
PBA3$^{+\bullet}$	−443.652 737	819.7	821.0	817.7
PBA4$^{+\bullet}$	−443.648 046	832.0	833.8	827.7

[a]Electronic energies (in hartree) are ZPE corrected.
[b]In kJ mol^{-1}.

the two families of conformers described above, particularly evident in the cases of 3-PPA and 4-PBA.

Moving from the neutral species to the radical cation, calculations show a distinct geometry change involving the NH_2 group. As already reported in the literature, when the amino group is devoid of an electron, it switches from tetrahedral to trigonal planar geometry.[8,34] This change clearly exhibits the site of the charge in the radical cations, mainly localized on the amino moiety in about any conformer. The calculated thermodynamic data clearly show that the presence of the amino group-π interaction in the case of radical cations strongly stabilizes the more folded structures of **PPA2$^{+\bullet}$** and **PBA2$^{+\bullet}$** with respect to **PPA1$^{+\bullet}$** and **PBA1$^{+\bullet}$**, by ca. 35 kJ mol^{-1}, according to the adopted computational method. The interaction involves the nitrogen atom of the amino group and the phenyl ring in a quite similar fashion as reported by the theoretical work by Deyà *et al.*[18] concerning the interaction between ionized ammonia and benzene. No effect is instead observed in the case of 2-PEA. In fact, the *gauche* structure **PEA2$^{+\bullet}$** is slightly less stable than the *anti*-one (**PEA1$^{+\bullet}$**), as already described by Metsala *et al.*[8] Any interaction between the ionized amino group and the ring is missing here, probably due to the geometric constraint imposed by the shorter length of the alkyl chain, which prevents an appropriate relationship between the two groups. A third optimized structure, **PEA3$^{+\bullet}$**, where the amino group is directed toward the ring, presents peculiar structural features when compared to **PEA1$^{+\bullet}$** and **PEA2$^{+\bullet}$**. The NH_2 group is, in fact, almost tetrahedral suggesting an important charge transfer from the amino to the phenyl group. This species is 21 kJ mol^{-1} less stable than **PEA1$^{+\bullet}$** at the CBS-QB3 level. The tetrahedral geometry at the alkylamino nitrogen placed 2.58 Å above an ortho ring carbon is rather reminiscent of the NH_3–ionized benzene adduct, rather complying to covalent bond formation as evidenced by an analysis of vibrational features.[35,36] It is worthwhile noting that the difference in energy between conformers **PEA1$^{+\bullet}$** and **PEA3$^{+\bullet}$** cannot be explained solely by the stabilization given by the methylene units in the *anti*-conformation. In fact, the *gauche* conformer **PEA2$^{+\bullet}$**, where the amino group is not interacting with the ring, is just 2.6 kJ mol^{-1} higher in energy. The extensive computational exploration of radical cations interacting with aromatic rings by Deyà *et al.*[18] has shown an important electron transfer from the amino group to the π-system when radical cations interact with benzene. This phenomenon is likely playing a role also in the present systems. We analyzed the singly occupied molecular orbital (SOMO) and the spin density of the PAA radical cations in order to ascertain the extent of electron transfer to the amino group from the ring. The SOMO and spin density isosurfaces are reported in Fig. 5 and Fig. S3 of the supplementary material, respectively. The spin density isosurface displays the same profile as the SOMO one, as expected. From the analysis of computed molecular orbitals, the interaction of the amino radical cation with the aryl group results in a significant electron transfer, particularly in the compact conformers of ionized 3-PPA and 4-PBA. When the amino group is far from the aryl, instead, different behaviors are found depending on the number of methylene units in the selected PPA. Specifically, in the radical cations of 2-PEA and 3-PPA, a certain delocalization of the SOMO on the aryl group is evidenced, even when the methylene groups are in all *anti*-arrangement. This effect stabilizes **PEA1$^{+\bullet}$**, **PEA2$^{+\bullet}$**, and **PPA2$^{+\bullet}$** conformers and can partly contribute to the peculiar behavior of 2-PEA. In fact, while the conformer **PEA1$^{+\bullet}$** presents the methylene units in the favored *anti*-conformation and the SOMO somewhat delocalized on the

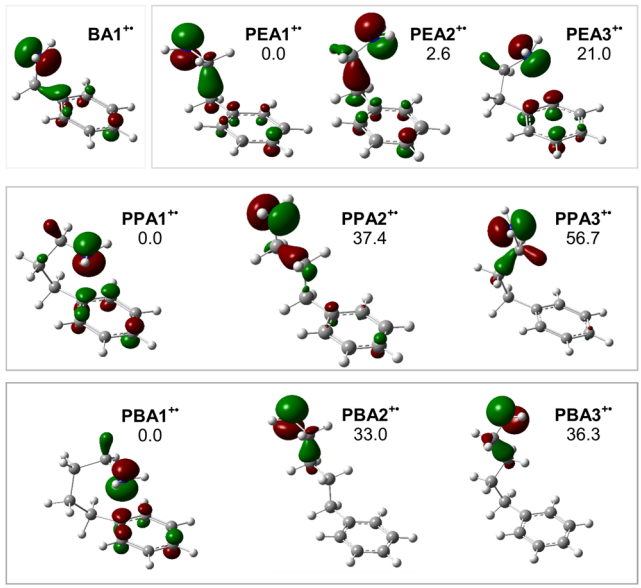

FIG. 5. Singly occupied molecular orbitals computed for representative radical cations of the assayed PAAs are plotted using an isovalue of 0.08. Relative ZPE corrected electronic energies calculated at the CBS-QB3 level are reported in kJ mol^{-1}.

aryl group, **PEA3**$^{+\bullet}$ shows eclipsed CH_2 groups and electron transfer to the amino radical cation from the benzene orbital, underlying the peculiar interaction between the amino nitrogen and the ortho ring carbon holding a major fraction of spin density. Comparing **PPA2**$^{+\bullet}$ and **PPA3**$^{+\bullet}$ is also interesting. The former conformer is, in fact, more stable by ca. 20 kJ mol^{-1} probably due to the contribution of the delocalized SOMO.[18] In the species with the longest alkyl chain (4-PBA), instead, there is almost no contribution to the stabilization of the molecular radical cation due to spin delocalization. In fact, the difference in energy between **PBA2**$^{+\bullet}$ and **PBA3**$^{+\bullet}$ is only 3 kJ mol^{-1}.

C. Computed versus experimental ionization energies

Insight into the information attached to the experimental IE values should rely on a survey of the photoionization transitions at play. We calculated for each conformer (their Boltzmann weighted fractions are reported in Fig. 4 in parentheses) the corresponding vertical ionization energy, assuming the Frank Condon approximation.[37–40] The energy of the radical cation was then calculated at the neutral geometry. These vertical IEs are reported in Table III. The agreement with the experimental IEs is meager though. The values are in fact leveled around an average value of ca. 8.90 eV, hardly displaying any trend with respect to variation in structure along the PPA series. Moreover the values of vertical IE are always higher with respect to the experimental data. This difference is absolutely reasonable since we expect that the experimental IEs will be closer to the theoretical adiabatic values than to the vertical ones.[21] Table III reports the adiabatic IEs representing the energy difference between each neutral conformer and the corresponding optimized radical cation, whose geometries are depicted in Fig. 4. As reported in previous studies,[41–43] the adiabatic IEs afford a more consistent matching with the experimental IEs, also listed in Table III. Thus, the experimental value of 8.54 ± 0.05 eV for BA is well accounted for by the theoretical IE of 8.50 eV for the **BA1** → **BA1**$^{+\bullet}$ transition. In the case of 2-PEA, the experimental IE of 8.37 ± 0.05 eV is in good agreement with the calculated values of 8.39 and 8.33 eV for the **PEA1** → **PEA2**$^{+\bullet}$ and for the **PEA2** → **PEA1**$^{+\bullet}$ transition, respectively. Both **PEA1** and **PEA2** are well represented conformers and the corresponding optimized radical cation structures involve relatively minor structural adjustments. For 3-PPA, the ionization of the most stable conformer, **PPA1** → **PPA1**$^{+\bullet}$, at 8.00 eV does not appear to contribute appreciably to the experimental value of 8.29 ± 0.05 eV. The reason is likely due to the considerable structural reorganization which accompanies leaning of the NH_2 group over the π-system, thus hampering the transition probability. Similarly, the **PPA4** → **PPA1**$^{+\bullet}$ transition at 7.94 eV suffers from a relatively minor frequency of the neutral conformer in the thermal population. The experimental value is instead rather well matched by the **PPA2** → **PPA2**$^{+\bullet}$ and **PPA3** → **PPA3**$^{+\bullet}$ transitions at 8.35 and 8.55 eV, respectively, both of them involving well represented conformers in the thermal population and requiring very minor structural rearrangement. In particular, the **PPA2** → **PPA2**$^{+\bullet}$ transition, delivering a radical cation with a largely delocalized SOMO embracing the π system, nicely accounts for the experimental value.

The 4-PBA case is another example where the lowest energy transition **PBA4** → **PBA1**$^{+\bullet}$ at 8.08 eV does not agree with the experimental IE of 8.31 ± 0.05 eV. This finding may be justified by the low abundance of **PBA4** in the conformer mixture. However, none of the alternative transitions presented in Table III, namely, **PBA2** → **PBA2**$^{+\cdot}$ at 8.46 eV, **PBA1** → **PBA3**$^{+\cdot}$ at 8.50 eV, and **PBA3** → **PBA4**$^{+\cdot}$ at 8.61 eV, can be reasonably discarded, all neutral conformers being well populated and turning into radical cations with only minor structural adjustments.

TABLE III. Calculated zero point corrected IEs at the CBS-QB3 level of selected conformers of ω-phenylalkylamines, obtained by comparing the energies of the neutral and radical cationic species. Experimentally determined IEs are also reported. All the energies are in eV.

Species	Experimental IE	Neutral	Radical	Vertical IE	Adiabatic IE
BA	8.54 ± 0.05[a]	**BA1**	**BA1**$^{+\bullet}$	8.95	8.50
2-PEA	8.37 ± 0.05[b]	**PEA1**	**PEA2**$^{+\bullet}$	8.98	8.39
		PEA2	**PEA1**$^{+\bullet}$	8.99	8.33
3-PPA	8.29 ± 0.05[c]	**PPA1**	**PPA1**$^{+\bullet}$	8.80	8.00
		PPA2	**PPA2**$^{+\bullet}$	8.92	8.35
		PPA3	**PPA3**$^{+\bullet}$	8.95	8.55
		PPA4	**PPA1**$^{+\bullet}$	8.94	7.94
4-PBA	8.31 ± 0.05	**PBA1**	**PBA3**$^{+\bullet}$	8.85	8.50
		PBA2	**PBA2**$^{+\bullet}$	8.93	8.46
		PBA3	**PBA4**$^{+\bullet}$	8.75	8.61
		PBA4	**PBA1**$^{+\bullet}$	8.95	8.08

[a]IE values previously reported in the literature include 8.49 ± 0.06 eV[44] and 8.8 eV,[45] as obtained by EI and photo-electron spectroscopy (PE), respectively.
[b]An IE value of 8.5 eV is reported (PE).[46]
[c]An IE value of 8.89 ± 0.12 eV is reported (PE).[46]

IV. CONCLUSIONS

Photoionization and photofragmentation energies of four linear ω-phenylalkylamines of increasing alkyl chain lengths were explored in the VUV region. The resulting IE values are 8.54 eV, 8.37 eV, 8.29 eV, and 8.31 eV for BA, 2-PEA, 3-PPA, and 4-PBA, respectively. Theoretical calculations run at the CBS-QB3 level allowed us to gain insight into the progressive reduction of IE values moving from BA to 3-PPA and 4-PBA. In particular, the computational survey has provided a detailed description on both electronic structure and geometric features regarding the radical cation conformers with the most appropriate geometry revealing radical cation–π interaction. The higher members of the PPA series, 3-PPA and 4-PBA, display a significant role of the radical cation-π interaction in affecting the stability of the folded conformers **PPA1**$^{+\bullet}$ and **PBA1**$^{+\bullet}$. However, this interaction, lowering the relative energy of the radical cation, requires a significant extent of structural rearrangement when the starting geometry corresponds to the thermally populated precursor neutral conformer, hampering both **PPA1**$^{+\bullet}$ and **PBA1**$^{+\bullet}$ to be in fact sampled with the adopted VUV photoionization mass spectrometry experiment.

The mass spectra of the selected phenylalkylamines were also acquired at a photon energy of 15 eV and the AEs of the most important fragments obtained from the PECs are

reported. The dissociation channel that leads to the formation of the $CH_2{=}NH_2^+$ fragment is by far the dominant path for all PAAs with the exception of BA for which hydrogen atom loss is largely prevailing.

Given the ubiquitous presence of the PAA scaffold in a variety of biomolecules, notably in the arylethylamino neurotransmitters, the present results may be relevant in understanding and predicting properties of these units in biological environments.

SUPPLEMENTARY MATERIAL

See supplementary material for photoionization efficiency plots of all the fragments reported in Table I and spin density isosurfaces of the sampled radical cations.

ACKNOWLEDGMENTS

The work was supported by Sapienza Università di Roma (Project No. C26H15MHLB) and by the European Community funding of the Gas Phase beamline of ELETTRA (Project No. 20150190).

[1] A. Bouchet, M. Schütz, B. Chiavarino, M. E. Crestoni, S. Fornarini, and O. Dopfer, Phys. Chem. Chem. Phys. **17**, 25742 (2015).
[2] S. Shaik, *Chemistry as a Game of Molecular Construction: The Bond Click Way* (Wiley, New Jersey, 2016).
[3] J. C. Lopez, V. Cortijo, S. Blanco, and J. L. Alonso, Phys. Chem. Chem. Phys. **9**, 4521 (2007).
[4] P. D. Godfrey, L. D. Hatherley, and R. D. Brown, J. Am. Chem. Soc. **117**, 8204 (1995).
[5] S. J. Martinez, J. C. Alfano, and D. H. Levy, J. Mol. Spectrosc. **158**, 82 (1993).
[6] J. A. Dickinson, M. R. Hockridge, R. T. Kroemer, E. G. Robertson, J. P. Simons, J. McCombie, and M. Walker, J. Am. Chem. Soc. **120**, 2622 (1998).
[7] J. Yao, H. S. Im, M. Foltin, and E. R. Bernstein, J. Phys. Chem. A **104**, 6197 (2000).
[8] R. Weinkauf, F. Lehrer, E. W. Schlag, and A. Metsala, Faraday Discuss. **115**, 363 (2000).
[9] P. R. Richardson, S. P. Bates, and A. C. Jones, J. Phys. Chem. A **108**, 1233 (2004).
[10] A. Golan, N. Mayorkas, S. Rosenwaks, and I. Bar, J. Chem. Phys. **131**, 024305 (2009).
[11] N. Mayorkas, S. Cohen, H. Sachs, and I. Bar, RSC Adv. **4**, 58752 (2014).
[12] B. Chiavarino, M. E. Crestoni, M. Schütz, A. Bouchet, S. Piccirillo, V. Steinmetz, O. Dopfer, and S. Fornarini, J. Phys. Chem. A **118**, 7130 (2014).
[13] M. Schütz, A. Bouchet, B. Chiavarino, M. E. Crestoni, S. Fornarini, and O. Dopfer, Chem. - Eur. J. **22**, 8124 (2016).
[14] M. Schütz, A. Bouchet, and O. Dopfer, Phys. Chem. Chem. Phys. **18**, 26980 (2016).
[15] R. Wu and T. B. McMahon, ChemPhysChem **9**, 2826 (2008).
[16] J. A. Stearns, S. Mercier, C. Seaiby, M. Guidi, O. V. Boyarkin, and T. R. Rizzo, J. Am. Chem. Soc. **129**, 11814 (2007).
[17] W. Fu, P. J. J. Carr, M. J. Lecours, M. Burt, R. A. Marta, V. Steinmetz, E. Fillion, T. B. McMahon, and W. S. Hopkins, Phys. Chem. Chem. Phys. **19**, 729 (2017).
[18] C. Estarellas, A. Frontera, D. Quiñonero, and P. M. Deyà, Phys. Chem. Chem. Phys. **13**, 16698 (2011).
[19] N. P.-A. Monney, T. Bally, G. S. Bhagavathy, and R. S. Glass, Org. Lett. **15**, 4932 (2013).
[20] D. W. Werst, J. Am. Chem. Soc. **113**, 4345 (1991).
[21] M. C. Castrovilli, P. Bolognesi, A. Cartoni, D. Catone, P. O'Keeffe, A. R. Casavola, S. Turchini, N. Zema, and L. Avaldi, J. Am. Soc. Mass Spectrom. **25**, 351 (2014).
[22] A. Derossi, F. Lama, M. Piacentini, T. Prosperi, and N. Zema, Rev. Sci. Instrum. **66**, 1718 (1995).
[23] M. C. Castrovilli, P. Bolognesi, A. Casavola, A. Cartoni, D. Catone, P. O'Keeffe, and L. Avaldi, Eur. Phys. J. D **68**, 253 (2014).
[24] K.-M. Weitzel, J. Mahnert, and M. Penno, Chem. Phys. Lett. **224**, 371 (1994).
[25] Spartan 10, Program for Calculation of Molecular Properties, Wavefunction, Inc., Irvine, CA, USA.
[26] M. J. Frisch, G. W. Trucks, H. B. Schlegel, G. E. Scuseria, M. A. Robb, J. R. Cheeseman, G. Scalmani, V. Barone, B. Mennucci, G. A. Petersson, H. Nakatsuji, M. Caricato, X. Li, H. P. Hratchian, A. F. Izmaylov, J. Bloino, G. Zheng, J. L. Sonnenberg, M. Hada, M. Ehara, K. Toyota, R. Fukuda, J. Hasegawa, M. Ishida, T. Nakajima, Y. Honda, O. Kitao, H. Nakai, T. Vreven, J. A. Montgomery, Jr., J. E. Peralta, F. Ogliaro, M. Bearpark, J. J. Heyd, E. Brothers, K. N. Kudin, V. N. Staroverov, R. Kobayashi, J. Normand, K. Raghavachari, A. Rendell, J. C. Burant, S. S. Iyengar, J. Tomasi, M. Cossi, N. Rega, J. M. Millam, M. Klene, J. E. Knox, J. B. Cross, V. Bakken, C. Adamo, J. Jaramillo, R. Gomperts, R. E. Stratmann, O. Yazyev, A. J. Austin, R. Cammi, C. Pomelli, J. W. Ochterski, R. L. Martin, K. Morokuma, V. G. Zakrzewski, G. A. Voth, P. Salvador, J. J. Dannenberg, S. Dapprich, A. D. Daniels, Ö. Farkas, J. B. Foresman, J. V. Ortiz, J. Cioslowski, and D. J. Fox, GAUSSIAN 09, Revision D.01, Gaussian, Inc., Wallingford, CT, 2009.
[27] J. A. Montgomery, Jr., M. J. Frisch, J. W. Ochterski, and G. A. Petersson, J. Chem. Phys. **112**, 6532 (2000).
[28] G. P. F. Wood, L. Radom, G. A. Petersson, E. C. Barnes, M. J. Frisch, and J. A. Montgomery, Jr., J. Chem. Phys. **125**, 094106 (2006).
[29] M. Xie, Z. Zhou, Z. Wang, D. Chen, and F. Qi, Int. J. Mass Spectrom. **303**, 137 (2011).
[30] R. Ruede, H. Troxler, C. Beglinger, and M. Jungen, Chem. Phys. Lett. **203**, 477 (1993).
[31] J. H. Catanzarite, Y. Haas, H. Reisler, and C. Wittig, J. Chem. Phys. **78**, 5506 (1983).
[32] S. G. Lias, "Ionization energy evaluation," in *NIST Chemistry WebBook: NIST Standard Reference Database Number 69*, edited by P. J. Linstrom and W. G. Mallard (National Institute of Standards and Technology, Gaithersburg, MD), retrieved December 15, 2017, http://webbook.nist.gov.
[33] J. M. Dyke, E. P. F. Lee, and M. H. Z. Niavaran, Int. J. Mass Spectrom. Ion Processes **94**, 221 (1989).
[34] M. N. R. Ashford, R. N. Dixon, R. J. Stickland, and C. M. Western, Chem. Phys. Lett. **138**, 201 (1987).
[35] K. Mizuse, A. Fujii, and N. Mikami, J. Phys. Chem. A **110**, 6387 (2006).
[36] K. Mizuse, H. Hasegawa, N. Mikami, and A. Fujii, J. Phys. Chem. A **114**, 11060 (2010).
[37] J. H. Gross, in *Mass Spectrometry*, 2nd ed. (Springer-Verlag, Berlin, Heidelberg, 2011), Chap. 2, p. 21.
[38] R. Seiler, Int. J. Quantum Chem. **3**, 25 (1969).
[39] R. H. Lipson, "Ultraviolet and visible absorption spectroscopy," in *Encyclopedia of Applied Spectroscopy*, edited by D. L. Andrews (Wiley-VCH, Berlin, 2009), Chap. 11, p. 353.
[40] J. Franck, Trans. Faraday Soc. **21**, 536 (1925).
[41] L. Wei, B. Yang, J. Wang, C. Huang, L. Sheng, Y. Zhang, F. Qi, C.-S. Lam, and W.-K. Li, J. Phys. Chem. A **110**, 9089 (2006).
[42] R. Sun, Q. Meng, M. Wang, W. Fei, Y. Zhang, J. Chen, W. Fang, X. Shan, F. Liu, and L. Sheng, J. Phys. B: At., Mol. Opt. Phys. **50**, 235101 (2017).
[43] C. Joblin, L. Dontot, G. A. Garcia, F. Spiegelman, M. Rapacioli, L. Nahon, P. Parneix, T. Pino, and P. Bréchignac, J. Phys. Chem. Lett. **8**, 3697 (2017).
[44] E. T. Selim, M. A. Rabbih, and M. A. Fahmey, Org. Mass Spectrom. **22**, 381 (1987).
[45] D. H. Aue and M. T. Bowers, "Stabilities of positive ions from equilibrium gas phase basicity measurements," in *Ions Chemistry*, edited by M. T. Bowers (Academic Press, New York, 1979), Chap. 9.
[46] L. N. Domelsmith, L. L. Munchausen, and K. N. Houk, J. Am. Chem. Soc. **99**, 4311 (1977).